

Catalytic and biological valorization of a supramolecular mononuclear copper complex based 4-aminopyridine

Nabil Hfidhi¹ | Intidhar bkhairia² | Dhieb Atoui³ | Jaurusup Boonmak⁴ | Moncef Nasri² | Ridha Ben Salem³ | Sujittra Youngme⁴ | Houcine Naïli¹

¹Laboratoire Physico-chimie de l'Etat Solide, Département de Chimie, Faculté des Sciences de Sfax, Université de Sfax, B. P. 1171, 3000 Sfax, Tunisia

²Laboratory of Enzyme Engineering and Microbiology, University of Sfax, National School of Engineering of Sfax (ENIS), Tunisia

³Organic Chemistry Laboratory (LR17/ES08), University of Sfax, Faculty of Sciences of Sfax, Tunisia

⁴Materials Chemistry Research Center, Department of Chemistry and Center of Excellence for Innovation in Chemistry, Faculty of Science, Khon Kaen University, Khon Kaen 40002, Thailand

Correspondence

Houcine Naïli, Laboratoire Physico-chimie de l'Etat Solide, Département de Chimie, Faculté des Sciences de Sfax, B.P. 1171, 3000 Sfax, Université de Sfax, Tunisia.

Email: houcine_naïli@yahoo.com

Hydrothermal reaction of copper bromide with 4-aminopyridine in DMF solution yields a new mononuclear copper complex $[\text{Cu}(\text{C}_5\text{H}_6\text{N}_2)_4]2\text{Br}\cdot 2(\text{C}_3\text{H}_7\text{NO})$ abbreviated **Cu-4AP-Br**. The product was characterized, structurally, by single-crystal X-ray diffraction analysis and, thermally, by DSC-ATG measurement. The inorganic–organic hybrid compound **Cu-4AP-Br** crystallizes in the centrosymmetric space group *Pbcn*, exhibiting a supramolecular network. Simultaneous DSC-ATG analysis shows that this compound remains stable up to 100 °C and then performs a successive decompositions accompanied with endothermic peaks. The complex **Cu-4AP-Br** was applied as a catalyst in the Heck coupling reaction under ultrasonic irradiation in various reaction conditions. The yields, obtained for a short period of time, allow us to consider this complex, generating selectivity on the external position of styrene with a preference of the *trans* form over *cis*, as an excellent catalyst for this type of reaction. Interestingly, **Cu-4AP-Br** displayed important antibacterial (Gram-positive and Gram-negative) and antioxidant activities (β -carotene bleaching inhibition, scavenging effect on DPPH free radical, and reducing power).

KEYWORDS

biological activities, crystal structure, heck coupling reaction, supramolecular, ultrasound

1 | INTRODUCTION

Transition metal complexes with a pyridine derivative ligand, as supramolecular hybrid inorganic–organic materials, have been gaining momentum owing to their enormous structural varieties and the accompanying multitude of potential applications in various fields, including catalysis, photochemistry, magnetism and biotechnology.^[1–5] Their impressive compositional diversities and versatile applications have extensively driven continuous interest in designing and making novel transition metals complexes-based functional materials. It is now well established that the structure, the dimensionality and the properties of these

supramolecular materials are depending on both the nature of the inorganic centre (geometry, electronic configuration, reactivity, coordination number, etc.) and the structure of the organic molecule (shape, number and type of reactive functional groups). The development of new solid-state structures, which involve the self-assembly of molecules into well-defined supramolecular via noncovalent, multiple intermolecular interactions, showed the diversity of such materials in terms of structure, topology and composition.^[6–10] The bonding in these materials is just as diverse as their structures, with covalent, ionic, and coordination bonds, hydrogen bonding, van-der Waals (vdW) forces, and $\pi\cdots\pi$ stacking, being observed in a single compound. On the other

hand, copper (II) is a typical transition metal ion characterized by its ability to form a wide range of coordination complexes, incorporating octahedral, tetrahedral and square-coplanar along with many kinds of irregular coordination geometries and, thus offering a good structure diversity. The geometry of the coordination polyhedron around copper (II) is also influenced by several subtle ligand factors, such as ligand constraints and steric hindrance.

A large number of these complexes were applied as catalysts that allow to synthesize new target molecules such as natural products and pharmaceutical compounds. Some current studies focus on examining copper owing to its low cost and abundance compared to other transition metals.^[11] These tests reveal that copper can have an excellent catalytic activity and better selectivity in catalytic reactions such as oxidation,^[12] epoxidation^[13] and polymerization.^[14] In the same context, Kocovsky *et al.*^[15] reported that copper complexes with sterically hindered nitrogen ligands are excellent catalysts. These complexes are stable and more active than those of phosphine ligands.

On the other hand, the increasing interest of researchers for chemical modification of biologically active compounds by complexation with various metals is noteworthy.^[16] New therapeutic strategies based on agents sharing antioxidant, anti-microbial and anti-inflammatory properties should be helpful to counter the development of chronic diseases. As an extension of this study and in an attempt to establish structure-activity relationships, it seemed of interest to further investigate the biological aspects of the synthesized compound. It is known that various substances, containing pyridine derivatives molecules, exhibit antibacterial activity.^[17] Furthermore, metal ions of the first transition series, such as copper, possess a certain degree of antioxidant,^[18] which can provide an additional mechanistic pathway of its anti-tumor action.^[19] Recently Ji *et al.*^[20] reported that a series of compounds based on Copper (II) represent an important biological activity and would be good candidates to be used for medical practice. Some organically template copper have been used as inhibitors of HIV-1 protease,^[21] antibacterial and antioxidant activities,^[22] and antitumor properties.^[23]

With respect to our investigations pertaining to the mononuclear copper complex, we report, herein, the chemical preparation, the thermal behavior, the biological activities, the crystallographic description and the catalytic properties of $[\text{Cu}(\text{C}_5\text{H}_6\text{N}_2)_4]2\text{Br}\cdot 2(\text{C}_3\text{H}_7\text{NO})$ in the Heck cross-coupling reaction under ultrasonic irradiation. This activation method proved to be ecological, highly quick and efficient in terms of

improving the evolution and the selectivity of the chemical reaction.

2 | MATERIALS AND METHODS

2.1 | Materials

All the solvents and chemicals were of reagent grade quality. They were purchased from commercial sources and used as received.

2.2 | Synthesis

A mixture of CuBr_2 (0.22 g, 1 mmol) and 4-aminopyridine (0.27 g, 3 mmol) in 5 ml of N,N-Dimethylformamide (DMF) was transferred to a stainless steel autoclave, sealed and placed in a programmable stove. The temperature was raised to 140 °C at 5 deg/min and held at that temperature for 24 hr, then cooled at 0.1 deg/min to 90 °C and held for 12 hr; afterwards it was cooled at the same rate to 70 °C and held for another 12 hr, and finally cooled down to room temperature at 0.1 deg/min (Figure 1). The resulting plate purple crystals of $[\text{Cu}(\text{C}_5\text{H}_6\text{N}_2)_4]\text{Br}_2\cdot 2(\text{C}_3\text{H}_7\text{NO})$ were collected, washed with ethanol and then air dried.

2.3 | X-ray data collection and structure determinations

Details of crystallographic data collection and refinement parameters for the complex **Cu-4AP-Br** are shown in Table 1. A single crystal, of dimensions 0.37*0.31*0.25 mm, was mounted onto a MiTeGen MicroLoops 200 μm . Diffraction intensities for complex **Cu-4AP-Br** were collected on Bruker D8 Quest

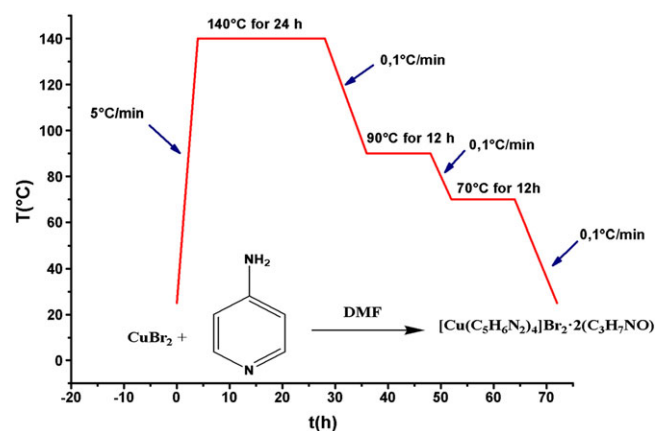


FIGURE 1 The reaction scheme with the different steps to synthesis the Cu-4AP-Br complex

TABLE 1 Crystallographic data of *Cu-4AP-Br*

Structural parameter	Compound (1)
Formula	[Cu(C ₅ H ₆ N ₂) ₄]Br ₂ ·2(C ₃ H ₇ NO)
Formula weight (g mol ⁻¹)	746.02
Temperature (K)	298 K
Crystal system	Orthorhombic
Space group	<i>Pbcn</i>
A (Å)	10.8139(11)
b (Å)	15.8635(15)
c (Å)	19.1580(12)
Volume (Å ³)	3286.5(6)
Z	4
Diffractometer	Bruker D8 Quest PHOTON100 CMOS
ρ _{cal} (mg m ⁻³)	1.508
Absorption correction	Multi-scan
Crystal size (mm ³)	0.37 x 0.31 x 0.25
Crystal color/shape	Purple, Plate
μ (mm ⁻¹)	3.14
θ range (deg)	θ _{min} = 2.8; θ _{max} = 26.4
hkl range	-13 ≤ h ≤ 12 -19 ≤ k ≤ 17 -23 ≤ l ≤ 23
No. of reflections collected	3357
No. of independent reflections	1306
F (000)	1516.0
R1	0.0686
wR2	0.1438
GooF	0.983
Transmission factors	T _{min} = 0.769, T _{max} = 0.837
Largest difference map hole (e Å ⁻³)	Δρ _{min} = -0.39; Δρ _{max} = 0.43

PHOTON100 CMOS diffractometer, equipped with graphite-monochromated MoK α radiation with radiation wavelength 0.71073 Å by using the φ - ω scan technique at ambient temperature. Data collection, cell refinement, data reduction and analysis were carried out by means of the APEX2 program.^[24] Analytical absorption correction was applied to the data with the use of SADABS.^[24] The structure was solved by direct methods and refined with the full-matrix least-squares technique, using SHELXS-97 and SHELXL-97 programs.^[25] Anisotropic thermal parameters were assigned to all non-hydrogen atoms. The organic hydrogen atoms were generated geometrically. All the figures were designed using DIAMOND program.^[26]

2.4 | Thermal analysis measurements

DSC-ATG measurements of *Cu-4AP-Br* were performed using a ASDT Q600 instrument, under air flow (100 ml/min), with a heating rate of 5 °C min⁻¹ up to 900 °C.

2.5 | General procedure for the catalytic activity studies

2.5.1 | Experimental

0.01 mmol of catalyst, 3 mmol of base, 2 mmol of aryl halide, 2.5 mmol of styrene and 6 ml of the solvent were introduced successively in the reactor (glass bottle) and subjected to ultrasonic irradiation. After the reaction, the resulting mixture was cooled and the organic phase extracted by means of diethyl ether. Subsequently, the reaction crude was purified by column of silica with 80% of n-hexane and 20% of dichloromethane as eluent to yield the final product.

2.5.2 | Characterization

Gas chromatographic (GC) analyses were performed by a Shimadzu GC-2014 device, to which a WBI-2014 injector and a FID-2014 detector were connected with a DB-5 capillary column. The carrier gas was nitrogen. All analyses were processed using GC-solution software.

The ¹H NMR and ¹³C NMR spectra of the synthesized compounds were recorded on a Bruker AC 400 apparatus with Fourier transform and a nominal frequency of 100 MHz. Chemical shifts were expressed in parts per million (ppm) relative to tetramethylsilane (TMS), used as an internal reference. The spectra were recorded in chloroform-d.

FT-IR spectra were recorded by a PerkinElmer Spectrum 100 apparatus. The absorption frequencies (ν) were expressed in cm⁻¹.

The ultrasonic activation was affected by an ultrasonic device (model Sonopuls HD 3200, 20 kHz, 200 W) coupled to an ultrasonic generator (Sonics VC 505, 300 W) and an ultrasonic probe (MS-72, Φ = 2 mm).

2.5.3 | (E)-stilbene

IR (KBr, cm⁻¹) ν = 3128–2837 (CH aro), 1500 (C=C ethyl), 1449 (C=C aro), 963 (CH ethyl); ¹H NMR (400 MHz, CDCl₃) δ (ppm) = 7.54 (d, 4H, J = 7.52 Hz), 7.40 (t, 4H, J = 7.39 Hz), 7.30–7.24 (m, 2H), 7.15 (s, 2H); ¹³C NMR (100 MHz, CDCl₃) δ (ppm) = 137.36, 128.72, 128.69, 127.63, 126.53.

2.5.4 | (Z)-stilbene

IR (KBr, cm^{-1}) $\nu = 3146\text{--}2843$ (CH aro), 1537 (C=C ethyl), 1361 (C=C aro), 1106 (CH ethyl); ^1H NMR (400 MHz, CDCl_3) δ (ppm) = 7.53 (d, 4H, $J = 7.53$ Hz), 7.37 (t, 4H, $J = 7.38$ Hz), 7.32–7.21 (m, 2H), 7.13 (t, 2H, $J = 7.14$ Hz); ^{13}C NMR (100 MHz, CDCl_3) δ (ppm) = 137.45, 128.82, 127.77, 126.65.

2.6 | In vitro biological activities

2.6.1 | Antioxidant activities

β -carotene bleaching assay

The ability of **Cu-4AP-Br** to prevent the bleaching of β -carotene was assessed as described by Koleva *et al.*^[27] A stock solution of β -carotene/linoleic acid mixture was prepared by dissolving 0.5 mg of β -carotene, 25 μl of linoleic acid and 200 μl of Tween 40 in 1 ml of chloroform. The chloroform was completely evaporated under vacuum in a rotatory evaporator at 40 °C, then 100 ml of bi-distilled water were added, and the resulting mixture was vigorously stirred. The emulsion obtained was freshly prepared prior to each experiment. Aliquots (2.5 ml) of the β -carotene/linoleic acid emulsion were transferred to test tubes containing 0.5 ml of **Cu-4AP-Br** solution (0.1 to 1 mg/ml). The tubes were immediately placed in water bath and incubated at 50 °C for 2 hr. Finally, the absorbance of each sample was measured at 470 nm using a UV-Visible spectrophotometer (T70, UV/VIS spectrometer, PG Instruments Ltd., China). A blank was conducted in the same manner, except that distilled water was used instead of sample. The BHA was used as positive control. Three replicates were conducted for each test sample. The antioxidant activity was determined by:

$$\text{Antioxidant activity (\%)} = 1 - \frac{A_0}{A_0'} \cdot \frac{A_t}{A_t'} \times 100$$

where A_0 and A_0' are the absorbances of the sample and the blank, respectively, measured at time zero, and A_t and A_t' are the absorbances of the sample and the blank, respectively, measured after incubation for 2 hr.

Reducing power assay

The ability of **Cu-4AP-Br** to reduce iron (III) was determined according to the method of Yildirim *et al.*^[28] Sample (1 ml) at different concentrations (0.1 to 1 mg/ml) was mixed with 2.5 ml of 0.2 M phosphate buffer (pH 6.6) and 2.5 ml of $\text{K}_3\text{Fe}(\text{CN})_6$ solution (1% (w/v)). The mixtures were incubated for 30 min at 50 °C. After incubation, 2.5 ml of TCA (10% (w/v)) were added and the reaction mixtures were then centrifuged

for 10 min at $10,000 \times g$. Finally, 2.5 ml of the supernatant solution from each sample mixture were mixed with 2.5 ml of distilled water and 0.5 ml of FeCl_3 (0.1% (w/v)). After a 10-min reaction time, the absorbance of the resulting solutions was measured at 700 nm. The control was conducted in the same manner, except that distilled water was used instead of sample. BHA was used as reference antioxidant. Values presented are the mean of two analyses.

PPH radical-scavenging assay

DPPH radical-scavenging activity of **Cu-4AP-Br** was determined as described by Bersuder *et al.*^[29] Sample (500 μl) at different concentrations (0.1 to 1 mg/ml) was mixed with 375 μl of ethanol (99.5%) and 125 μl of DPPH (0.02%) in ethanol (99.5%). The mixtures were then kept at room temperature in the dark for 1 hr, and the reduction of DPPH radical was measured at 517 nm using a UV-Visible spectrophotometer (T70, UV/VIS spectrometer, PG Instruments Ltd., Beijing, China). When the DPPH radical was scavenged, the color of the reaction mixture changed from purple to yellow with the decrease of absorbance. The control was conducted in the same manner, except that DMSO was used instead of sample. The DPPH radical scavenging activity was calculated as follows:

$$\begin{aligned} \text{DPPH radical - scavenging activity (\%)} \\ = \frac{A_{\text{control}} - A_{\text{sample}}}{A_{\text{control}}} \times 100 \end{aligned}$$

where A_{control} is the absorbance of the control reaction and A_{sample} is the absorbance of sample reaction. BHA was used as a positive control. The test was carried out in duplicate and the results are mean values.

2.6.2 | Antibacterial activity

Microorganisms

Antibacterial activity of **Cu-4AP-Br** was tested against Gram positive and Gram negative bacterial strains. The bacteria used were *Staphylococcus aureus* (ATCC 25923), *Bacillus cereus* (ATCC 11778), *Enterococcus faecalis* (ATCC 29212), *Micrococcus luteus* (ATCC 4698), *Salmonella enterica* (ATCC 43972) and *Klebsiella pneumoniae* (ATCC 13883).

Agar-well diffusion method

Antibacterial test was performed by agar-well diffusion method as described by Tagg and McGiven (1971).^[30] A fresh cell suspension (200 μl) adjusted to 10^6 cfu/ml for bacteria was inoculated onto the surface of agar plates. Thereafter, wells with 6 mm in diameter were punched

in the inoculated agar medium with sterile Pasteur pipettes and 50 μL of **Cu-4AP-Br** in dimethylsulphoxide (DMSO) with a concentration of 2 mg/ml added to each well. The plate was allowed to stand for 4 hr at 4 $^{\circ}\text{C}$ to allow the diffusion of the extracts in the agar, followed by incubation at 37 $^{\circ}\text{C}$ for 24 hr.

The antimicrobial activity was evaluated by measuring the inhibition zone diameters (IZD) (including well diameter of 6 mm).

Anti-inflammatory activity

The anti-inflammatory activity was assessed using the spectrophotometric measurement of a conjugated diene, the result of linoleic acid oxidation by the enzyme 5-LOX.^[31] Briefly, 500 μL of buffer (pH = 7.4) (Na_2HPO_4 , $2\text{H}_2\text{O}$; KH_2PO_4 ; NaCl) were mixed with 200 μL of protein hydrolysate, 200 μL of linoleic acid and 100 μL of 5-LOX enzyme solution. The mixture was homogenized and incubated for 10 min at 25 $^{\circ}\text{C}$. The absorbance was determined at 234 nm against a blank. Naprosyn (NAP) was used as a standard.

3 | RESULTS AND DISCUSSION

3.1 | Crystal structure of $[\text{Cu}(\text{C}_5\text{H}_6\text{N}_2)_4]2\text{Br}\cdot 2(\text{C}_3\text{H}_7\text{NO})$

The new copper (II) complex **Cu-4AP-Br** crystallizes in the orthorhombic system with the centrosymmetric space group $Pbcn$. The lattice parameters are $a = 10.8139(11)$ \AA , $b = 15.8635(15)$ \AA , $c = 19.1580(12)$ \AA and the volume of the unit cell is $V = 3286.5(6)$ \AA^3 . A complete list of the structure factors is illustrated in Table 1. As demonstrated in Figure 2, the complex **Cu-4AP-Br** is generated by a two-fold rotation axis and consists of isolated tetraaminopyridine cuprate (II) cations $[\text{Cu}(\text{C}_5\text{H}_6\text{N}_2)_4]^{2+}$, free bromine anions $[\text{Br}^-]$ and uncoordinated solvent dimethylformamide molecules ($\text{C}_3\text{H}_7\text{NO}$) which are all connected by a complex hydrogen bond system to form a periodic 0 dimensional structure.

In this complex, the copper atom is located in a special position and coordinated by four nitrogen atoms of the pyridine ligand with $\text{Cu}-\text{N}$ bonds distance ranging from 2.003 (5) to 2.035 (8) \AA and $\text{N}-\text{Cu}-\text{N}$ angles varying from 88.47 (15) to 180.000 (3) $^{\circ}$ (Table 2). These values fall in the range reported previously for compounds containing $\text{Cu}-\text{N}$ bonds.^[32] Visual inspection of the molecular structure in Figure 2 reveals that the coordinated copper complex deviates substantially from a square-planar geometry. Thus, the degree of distortion of $[\text{Cu}(\text{C}_5\text{H}_6\text{N}_2)_4]^{2+}$ coordination polyhedral was determined by the index of tetrahedrality introduced by

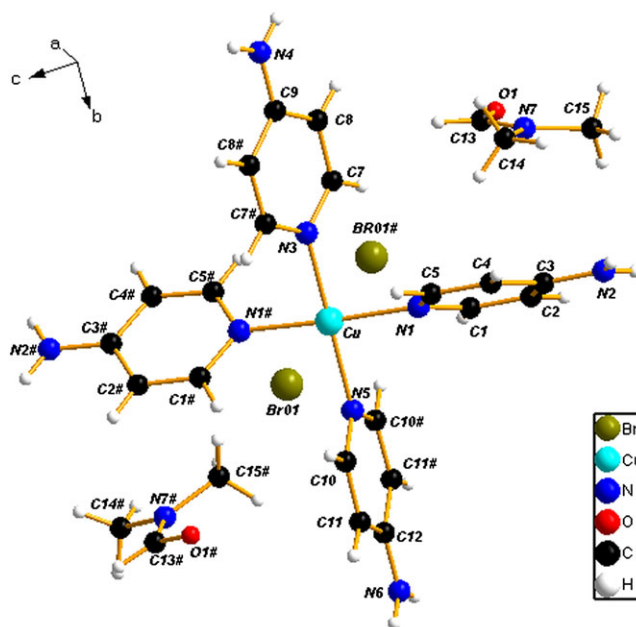


FIGURE 2 Asymmetric unit representation of $[\text{Cu}(\text{C}_5\text{H}_6\text{N}_2)_4]2\text{Br}\cdot 2(\text{C}_3\text{H}_7\text{NO})$ generated by the two-fold rotation axis along the crystallographic b axis

Addison and coworkers for a four coordinated complex,^[33] $\tau_4 = [360^\circ - (\alpha \pm \beta)]/141^\circ$ (α and β as the two largest angles ($\text{N}5-\text{Cu}-\text{N}3$ and $\text{N}1-\text{Cu}-\text{N}1\#$) in the four-coordinate species). The values of τ_4 range from 1 for a perfect tetrahedral geometry, since $360^\circ - 2(109.5^\circ) = 141^\circ$, to 0 for a perfect square-planar geometry, since $360^\circ - 2(180^\circ) = 0$. Calculated τ_4 parameter for **Cu-4AP-Br** is $0.021 \approx 0.00$, demonstrating that the cation $[\text{Cu}(\text{C}_5\text{H}_6\text{N}_2)_4]^{2+}$, exhibits a square planar (D_{4h}) geometry. In addition, the dihedral angle between the planes $\text{N}1\text{CuN}5$ and $\text{N}3\text{CuN}1\#$ is equals to 0° confirms the regular square-planar geometry of the CuN_4 entity and the planarity of the five atoms (Cu and the four $\text{N}_{\text{pyridine}}$ atoms). Indeed, copper atoms are separated from each other along the a , b and c crystallographic axis, with the shortest metal-metal distance equal to 9.599 (16) \AA , 10.813 (11) \AA and 11.192 (10) \AA , respectively, suggesting that they are very well isolated. This difference in the metal-metal distance is likely assigned to the size and the shape of the coordinated ligand.

On the other hand, the free Br^- anions are located above and below the square planar of $[\text{Cu}(\text{C}_5\text{H}_6\text{N}_2)_4]^{2+}$ with the $\text{Cu}\cdots\text{Br}$ distance equal to 3.537 (8) \AA , being too long to be considered as a coordinated bond. In fact, the electronic subshell d^9 of Cu (II) is responsible for the distortion of the copper coordination polyhedron and consequently generating an elongation of the $\text{Cu}\cdots\text{Br}$ bond. This phenomenon corresponds to the well-known Jahn-Teller effect. Indeed, in an octahedral field the five d -orbitals of the Cu ion split into two sets, labeled by symmetry as t_{2g} (d_{xy} , d_{yz} , d_{xz}) and e_g (d_{z^2} , $d_{x^2-y^2}$). The e_g

TABLE 2 Selected bond distances (Å) and angles (°) for **Cu-4AP-Br**

Cu—N1	2.003 (5)	C5—C4	1.361 (9)
Cu—N1 ⁱ	2.003 (5)	C8—C7	1.361 (9)
Cu—N3	2.013 (8)	C8—C9	1.394 (8)
Cu—N5	2.035 (8)	C9—C8 ⁱ	1.394 (8)
N5—C10 ⁱ	1.338 (8)	C1—C2	1.354 (9)
N5—C10	1.338 (8)	C3—N2	1.352 (8)
N3—C7	1.333 (8)	C3—C4	1.393 (9)
N3—C7 ⁱ	1.333 (8)	C3—C2	1.395 (9)
N1—C5	1.331 (8)	C12—C11 ⁱ	1.384 (8)
N1—C1	1.352 (9)	N4—C9	1.344 (12)
O1—C13	1.203 (9)	N7—C13	1.343 (9)
C11—C10	1.366 (9)	N7—C15	1.441 (10)
C11—C12	1.384 (8)	N7—C14	1.451 (9)
N6—C12	1.337 (11)	N4—C9—C8	121.8 (4)
N1—Cu—N1 ⁱ	176.9 (3)	N4—C9—C8 ⁱ	121.8 (4)
N1—Cu—N3	88.47 (15)	C8—C9—C8 ⁱ	116.4 (9)
N1 ⁱ —Cu—N3	88.47 (15)	N1—C1—C2	125.1 (7)
N1—Cu—N5	91.53 (15)	N3—C7—C8	124.2 (8)
N1 ⁱ —Cu—N5	91.53 (15)	N2—C3—C4	122.8 (7)
N3—Cu—N5	180.000 (3)	N2—C3—C2	121.2 (7)
C10 ⁱ —N5—C10	116.9 (9)	C4—C3—C2	116.0 (7)
C10 ⁱ —N5—Cu	121.6 (4)	C5—C4—C3	120.7 (7)
C10—N5—Cu	121.6 (4)	C1—C2—C3	119.2 (7)
C7—N3—C7 ⁱ	116.1 (9)	O1—C13—N7	123.9 (9)
C7—N3—Cu	121.9 (4)	C13—N7—C15	121.3 (7)
C7 ⁱ —N3—Cu	121.9 (4)	C13—N7—C14	121.9 (8)
C5—N1—C1	115.3 (6)	C15—N7—C14	116.7 (7)
C5—N1—Cu	122.4 (5)	N1—C5—C4	123.8 (7)
C1—N1—Cu	122.3 (5)	N5—C10—C11	122.9 (8)
C10—C11—C12	120.7 (7)	C7—C8—C9	119.6 (7)
N6—C12—C11 ⁱ	122.1 (4)	C11 ⁱ —C12—C11	115.8 (9)
N6—C12—C11	122.1 (4)		

Symmetry code: (i) $-x, y, -z + 3/2$.

orbitals are occupied by three electrons (d_{z^2} , $d_{x^2-y^2}$), giving rise to a doubly degenerate ground state and consequently the symmetry decreases by Jahn-Teller elongation along the c axis containing the bromine ions.^[34]

The presence of those halide atoms as a part of an anionic sublattice leads to a total negative charge of (2-) on the framework which is equilibrated by the presence of the cation $[\text{Cu}(\text{C}_5\text{H}_6\text{N}_2)_4]^{2+}$. The bromine atoms play a subordinate role in the stabilization of the structure.

Indeed, they participate in strong hydrogen bonds as acceptor with the amino groups [$\text{N2} \cdots \text{Br01} = 3.5370$ (61) Å, $\text{N4} \cdots \text{Br01} = 3.5086$ (41) Å and $\text{N6} \cdots \text{Br01} = 3.4908$ (40) Å].

In the title compound, the 4-aminopyridine ligand acts as a monodentate ligand by the ring nitrogen atom. The C-C and C-N bond lengths vary from 1.354 (9) Å to 1.395 (9) Å and 1.331 (8) Å to 1.352 (9) Å, respectively. The C-C-C and C-N-C bond angles fall in the range 115.8 (9)° to 120.7 (7)° and 118.7(7)° to 120.8(7)°, respectively. The main inter atomic distances and angles in the monodentate ligand are reported in Table 2. These values are in agreement with those observed in similar compounds.^[35] With regard the coordinated molecules are not in the same plane. The dihedral angles formed between these ligands in the *trans* position, are equal to 22.190° for $\text{N3}-\text{Cu}-\text{N5}$ and 59.718° for $\text{N1}-\text{Cu}-\text{N1}\#$.

The crystal structure of **Cu-4AP-Br** is stabilized by the hydrogen bonding interactions that involve the coordinated lattice 4-aminopyridine molecules as well as the bromine anions and DMF molecules. Furthermore, the supramolecular architecture of the title compound is built from the alternatively arranged cationic and anionic layers in wave forms along the crystallographic a axis (Figure 3). Moreover, the arrangement of the different species present in the lattice structure allows some dominant interactions, calculated by CRYSTAL EXPLORER,^[36] being H---H (47%), C---H/H---C (23%), H---Br/Br---H (18%), O---H/H---O (7%) and N---H/H---N (5%) (Figure 4), and thus generating a supramolecular network. These entities are interconnected significantly through extensive N—H---Br/O hydrogen bonding between the anionic and cationic moieties (Table 3) and C—H--- π stacking interactions between the aromatic rings of the amine molecules themselves. The uncoordinated bromide anion and DMF molecule play a significant role in providing the supramolecular aspect and form a connecting bridge between the isolated Cu-square planar themselves.

3.2 | Thermal analysis of $[\text{Cu}(\text{C}_5\text{H}_6\text{N}_2)_4]2\text{Br} \cdot 2(\text{C}_3\text{H}_7\text{NO})$

The thermal stability of **Cu-4AP-Br** crystal was studied by means of a simultaneous thermogravimetric analysis (TGA) and differential scanning calorimetric (DSC), carried out with a heating rate of 5 °C/min between 25 and 900 °C. The results are depicted in Figure 5. The TG curve illustrates that the compound is thermally stable up to 80 °C and the first mass loss starts above 80 °C due to the decomposition of two DMF molecules (observed weight loss, 18.8%; calculated weight loss, 19.58%). This

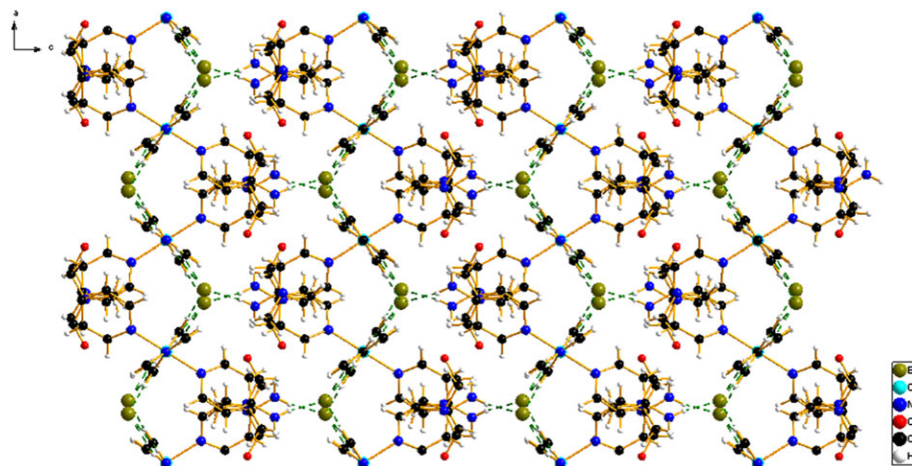


FIGURE 3 Projection of the structure along the crystallographic b-axis for compound Cu-4AP-Br, showing the supramolecular character and the alternation between the cationic and anionic parts in wave forms along the crystallographic a axis

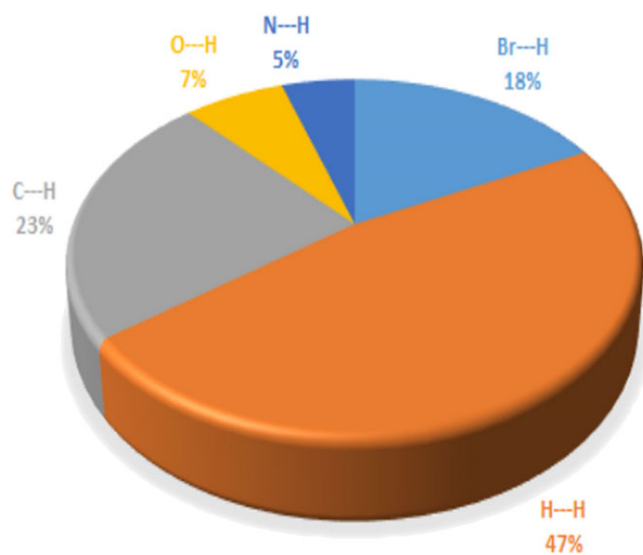


FIGURE 4 The pie chart of non-covalent interactions in Cu-4AP-Br

phenomenon is accompanied by an endothermic peak on the DSC curve after 80 °C. Furthermore, the second weight loss of 70.42%, observed on the TG curve in the temperature domain from 150 to 650 °C, is attributed to

the degradation of the organic molecules and one Br₂ molecule (calculated weight loss, 71.86%). This transformation is accompanied by endothermic peak at ~206 °C. The last transformation starts at about 650 °C and corresponds to the formation of copper oxide CuO as final residue (calculated weight loss, 89.28%; observed weight loss, 91.21%).

3.3 | Catalytic properties

The coupling reactions in the presence of complex based on transition elements are very interesting. They allow access to original syntheses of new compounds as pharmaceutical intermediates that can be used as medicaments. Generally, these reactions are carried out with a palladium catalyst.^[37,38] However, on account of their cost, toxicity and the instability of some palladium complexes,^[39,40] new transition metals such as ruthenium,^[41] nickel,^[42] manganese,^[43] cobalt,^[44] iron^[45] and copper^[46,47] have, recently, been examined.

In this work, we tested the complex **Cu-4AP-Br** as a catalyst in the coupling reaction of bromobenzene with

TABLE 3 Hydrogen-bond geometry (Å, °)

D—H...A	D—H	H...A	D...A	D—H...A
N6—HN6B...Br ⁱⁱ	0.86	2.63	3.491(4)	175.1
N6—HN6A...Br ⁱⁱⁱ	0.86	2.63	3.491(4)	175.1
N2—HN2A...Br ^{iv}	0.86	2.75	3.537(6)	153.5
N2—HN2B...O1 ^v	0.86	1.99	2.841(8)	171.9
N4—HN4B...Br ^v	0.86	2.69	3.508(4)	160.5
N4—HN4A...Br ^{vi}	0.86	2.69	3.508(4)	160.5

Symmetry codes: (ii) $x - 1, y + 1, z$; (iii) $-x + 1, y + 1, -z + 3/2$; (iv) $x - 1, -y + 1, z - 1/2$; (v) $x - 1, y, z$; (vi) $-x + 1, y, -z + 3/2$.

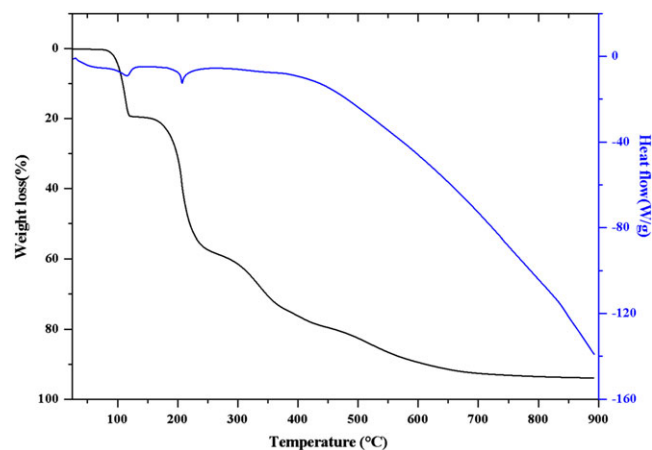


FIGURE 5 Simultaneous thermogravimetric analysis and differential scanning calorimetry scan for Cu-4AP-Br. The scan was performed in flowing air with a ramp rate of 5 °C/min

styrene, in the presence of different bases in various solvents (Figure 6) under ultrasonic irradiation using an MS-72 ultrasonic probe (diameter $\Phi = 2$ mm) immersed directly in the reaction mixture (Figure 7).

At first, we optimized the ultrasonic operating parameters. Thus, several parameters can be adjusted to influence the selectivity and the progress of the chemical reaction.^[48,49] The results obtained did not display any

progress of the reaction, whose amplitude is less than 30% (Table 4, entry 1–3), and then by increasing to 40% the yield decreases, which accounts for the threshold or the physical limit of ultrasonic activation. Therefore, the effect of ultrasound increases with the amplitude injected to a maximum value, which has the cavitation threshold. From this limit, cavitation becomes very intense. This increases the percentage of gas in the medium that decreases the effect of the ultrasonic waves since it is weakly driven by gas rather than a liquid.^[50]

The study of the pulsation period duration was affected by varying the ON/OFF times. To prevent the erosion of sonic emission surface horn, we relied on low durations, i.e. one to three seconds. The pulsating time in operation (t_E) is the duration of the emission of ultrasonic irradiation in the reaction medium during a period. Therefore, the effect of ultrasound increases with the creation of cavitations. On the contrary, the off pulsation 6+ time (t_A) designates the stop of the creation of the irradiation within the reaction mixture. During this period, the cavitations rate decreases, thus, decreasing the effects of the ultrasonic activation.

Based on the results obtained previously in our laboratory,^[51] we examined the bromobenzene coupling reaction with styrene catalyzed by **Cu-4AP-Br** in different

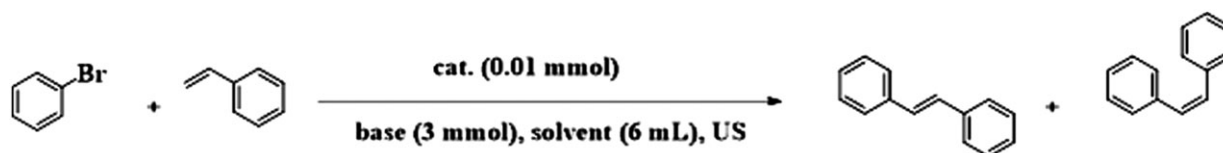


FIGURE 6 Heck reaction between bromobenzene and styrene

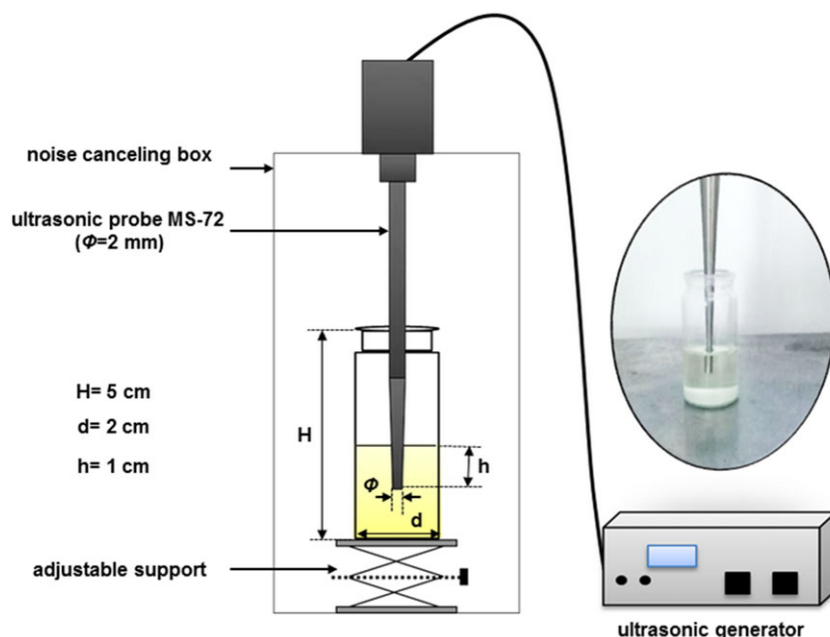


FIGURE 7 Mounting of the coupling reaction activated by ultrasonic irradiation

TABLE 4 Optimization of reaction parameters for Heck cross-coupling reaction of bromobenzene with styrene in the presence of **Cu-4AP-Br**

Entry	Amplitude (%)	$t_E - t_A^a$ (s)	solvent	base	Time(min)	Yield (%) ^b E/Z
1	15	2-2	DMF	Na ₂ CO ₃	45	No reaction
2	20	2-2	DMF	Na ₂ CO ₃	45	No reaction
3	25	2-1	DMF	Na ₂ CO ₃	45	No reaction
4	30	3-1	DMF	Na ₂ CO ₃	30	trace
5	35	3-2	DMF	Na ₂ CO ₃	60	99/<1
6	40	3-2	DMF	^t BuOK	120	65/<1
7	35	3-2	DMF	K ₂ CO ₃	60	99/<1
8	35	3-2	DMSO	Na ₂ CO ₃	60	100/none
9	35	3-2	MeCN	NaOH	90	73/26
10	35	3-2	MeCN	K ₂ CO ₃	90	72/26
11	35	3-2	MeCN	Na ₂ CO ₃	90	74/24
12	35	3-2	DMF	KOH	90	68/31
13	35	3-2	DMSO	Et ₃ N	60	82/16
14	35	3-2	DMSO	K ₂ CO ₃	60	99/<1
15	35	3-2	DMF	NaOH	60	79/20

(0.01 mmol) of catalyst, (2 mmol) of bromobenzene, (2.5 mmol) of styrene, (3 mmol) of base and 6 ml of the solvent under ultrasonic irradiation at 25 °C.

^aPeriod duration ($t = t_E + t_A$); t_E : pulsation time ON, t_A : pulsation time OFF.

^bThe yields were measured by GC using diethyl ether as solvent.

aprotic polar solvents. We chose DMF, DMSO and MeCN due to their high boiling temperatures to prevent their vaporization and to maintain the height (H) of reaction mixture (Figure 7). The obtained results are summarized in Figure 8.

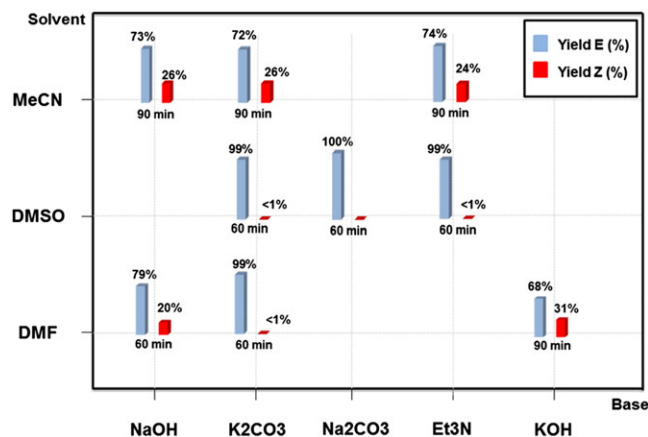
Among the three solvents tested, DMSO was the best solvent adapted to affect this type of coupling. Indeed, for a very short period of time (60 min), the progress of the reaction was almost total. In addition, an excellent selectivity on external position of styrene was noticed. In contrast, in the MeCN, the reaction time increases to

90 minutes with an average preference of the *trans* form over *cis*.

This is well confirmed in the presence of different bases such as NaOH, K₂CO₃ and Et₃N. In addition, we found that the reactivity of the reaction was increased by the addition of carbonate base. However, the use of NaOH or KOH increases the duration of the reaction and improves the *cis* form. This can confirm that the carbonate anions facilitate the reductive elimination step much more than the (OH⁻) ions.

In order to elucidate these results, we proposed the reaction mechanism presented in Figure 9. The proposed catalytic cycle starts with an oxidative addition accompanied by the release of one of four ligands 4-aminopyridine, which causes the formation of organocuprate (2).^[52] During this step, the degree of oxidation of copper increases by two units, according to a concerted mechanism, since the halogenated derivative is of Csp²-X type. The second step is the syn-insertion of styrene to the last complex (2) which results in the formation of a new C-C bond followed by stilbene removal and hydride (4). Finally, the corresponding base decomposes this hydride by trapping the HBr acid and the regeneration of Cu^{II}.

One of the most interesting advantages of this complex is its stability for air and temperature, favoring it to be a potential candidate for marketing; contrary to

**FIGURE 8** Solvent and base effects on the evolution and selectivity of the Heck reaction catalyzed by Cu-4AP-Br

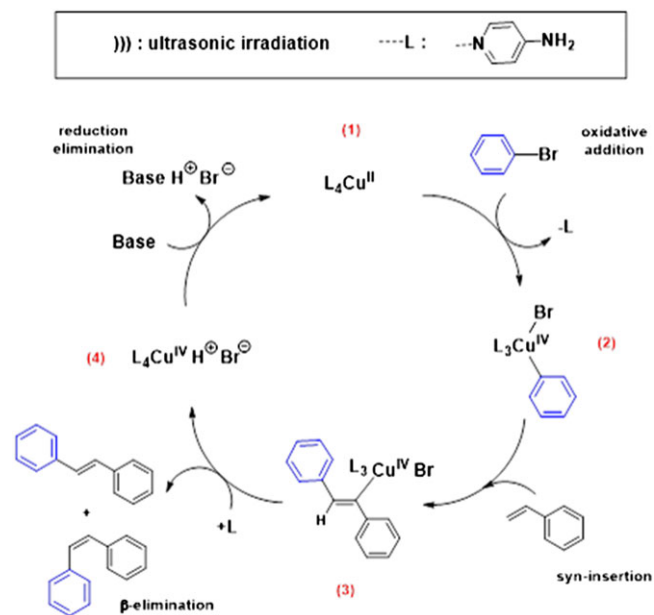


FIGURE 9 Cycle catalytic plausible of the Heck reaction catalyzed by Cu-4AP-Br

phosphine ligand complexes that need specific conditions during storage.^[53] Furthermore, this complex does not require any agent or additive to activate the reaction. Besides, a very remarkable selectivity of external arylation of styrene compared to complexes based on phosphine or oxygenated ligands was used in literature.^[54] From an ecological perspective, this complex verified certain principles of green chemistry. The yields found reveal that **Cu-4AP-Br** can replace palladium, the metal of choice for coupling reactions. This allows reducing the cost of the reaction and avoiding the paradox of synthesizing stilbene derivatives with anticancer activities^[55] using palladium complexes that can cause cancer.^[56]

To sum up, this complex is endowed with a stability, a reactivity and a well-defined selectivity that allow it to be, together with its ecological features, a new procedure in fine chemistry.

3.4 | Evaluation of *in-vitro* biological activity.

3.4.1 | Antioxidant activity

For many years, a large number of researches have actively investigated copper compounds based on the assumption that these endogenous metals may be less toxic. It has been established that the properties of copper-coordinated compounds are largely determined by the nature of ligands and donor atoms bound to the metal ion.^[57] Accordingly, we attempted to evaluate the

antioxidant capacity of the new elaborated complex **Cu-4AP-Br**. Its capacity was determined, *in vitro*, by means of β -carotene bleaching test, reducing power assay and DPPH scavenging ability.

β -carotene-linoleic acid assay

In this antioxidant test, the oxidation of linoleic acid generates free radicals, such as hydroperoxides which attack the highly unsaturated β -carotene molecules. When this reaction occurs and in the absence of antioxidants, the β -carotene molecule loses its conjugation and, therefore, β -carotene undergoes a rapid discoloration reaction. Antioxidant activity was determined by measuring the inhibition effects of **Cu-4AP-Br** and BHA to β -carotene bleaching. As shown in Figure 10, **Cu-4AP-Br** antioxidant activities in β -carotene-linoleate model system increased in a dose-dependent manner, however, it was lower than that of BHA. As noted in Figure 10, **Cu-4AP-Br** inhibits the oxidation of β -carotene with a 1% of $72.86 \pm 1.4\%$, at a concentration of 200 $\mu\text{g/ml}$. The antioxidant effect in the synthesized compound can reduce the extent of β -carotene destruction by neutralizing the linoleate-free radical and other free radicals formed in the system.

Free radical scavenging activity using DPPH assay

DPPH provides an easy and rapid method for the determination of antioxidant activity of synthesized compounds, since DPPH can directly react with the antioxidant species.^[58] The principle of the DPPH assay is a single electron transfer (SET) reaction and a hydrogen-atom removal.^[59] In our study, the metal complex compound showed good activities as a radical scavenger (Figure 11). It can be inferred that free radical scavenging activities of synthesized compound are

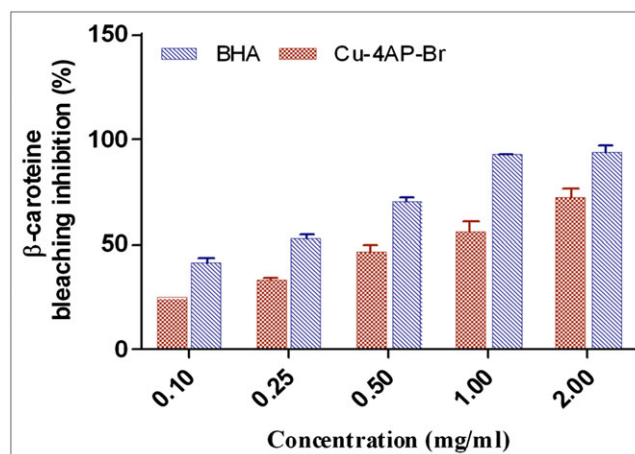


FIGURE 10 β -carotene bleaching activity of Cu-4AP-Br at different concentrations. BHA was used as positive control. Each experiment was executed in triplicate

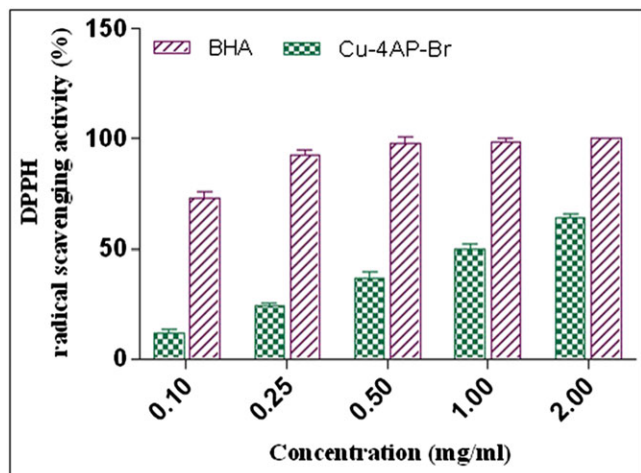


FIGURE 11 Scavenging effect on DPPH free radical of Cu-4AP-Br at different concentrations. BHA was used as positive control. Each experiment was executed in triplicate

concentration dependent. Correspondingly, Hazra *et al.*^[60] have indicated that all the metal complexes showed comparable or slightly less activity compared to that of standard. At concentrations range 10 to 200 $\mu\text{g/ml}$, **Cu-4AP-Br** was able to scavenge DPPH radicals and the value of the maximum inhibition was $63.91 \pm 1.08\%$. The obtained results were in agreement with several works reported in the literature with regards to the antioxidant potential of metal complexes. In a recent study, Sulpizio *et al.*^[61] have reported that the metal complexes [Cu (ISO)₂] and [Zn (ISO)₂] show 72 and 88% inhibition of the DPPH radical.

According to results of Saïd *et al.*,^[5] copper complex displayed significantly higher DPPH activity. Konarikova *et al.*, (2013)^[62] have also reported that, after complexation with metal ions, the antioxidant activity increases due to the presence of positively charged metal ions as well as electron donating groups present in the moiety. Thus, the complex compound has a strong potential to be applied as a scavenger to eliminate radicals.

Reducing power activity using FRAP assay

Reducing power also increased with the increase of **Cu-4AP-Br** and BHA concentration, and the values obtained for the synthesized compound were excellent, despite being about 69% of that of BHA (Figure 12). At 100 $\mu\text{g/ml}$, the absorbance value of **Cu-4AP-Br** is above 1.0. This result was similar to a previous study reporting that synthesized compounds (Itaconic anhydride (ITA)) exhibited high reducing power potential.^[63] It has been reported that the reducing properties are generally associated with the presence of reductones, shown to exert antioxidant action by donating a hydrogen atom and breaking the free radical chain.^[64]

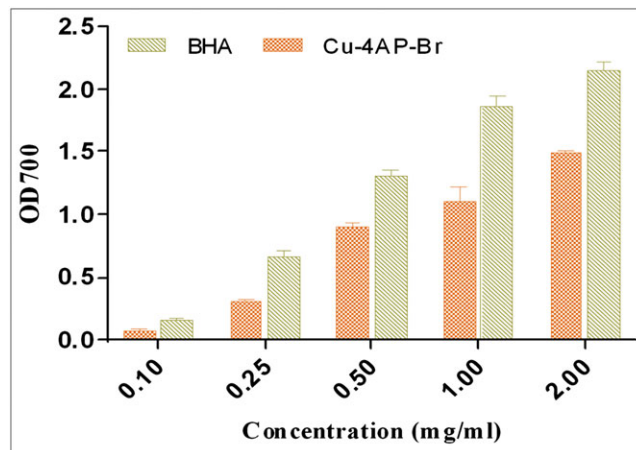


FIGURE 12 Reducing power of Cu-4AP-Br at different concentrations. BHA was used as positive control. Each experiment was executed in triplicate

3.4.2 | In-vitro antimicrobial activity of u-4AP-Br synthesized compound

From the industrial perspective, the organic compounds used for the purpose of disinfection are limited due to their toxicity towards healthy cells and instability at high temperatures and pressures.^[65] Hence, we are at the cutting edge stage of finding the alternative effective agent to deactivate microorganisms. Correspondingly, the synthesized compound **Cu-4AP-Br** is of high significance.

Antibacterial activity of **Cu-4AP-Br** complex was assessed against five strains. The result was compared with those of the standard (Bacitracin) and the mean diameters of inhibition zones are shown in Table 5. Based on the results, it can be concluded that the synthesized **Cu-4AP-Br** has significant antibacterial action against both of the Gram classes of bacteria. **Cu-4AP-Br** exhibits intermediate to higher bioactivity against all organisms and its activity is promising toward *Salmonella enterica*. At a concentration of 200 $\mu\text{g/ml}$, antimicrobial activities of **Cu-4AP-Br** against *Micrococcus luteus*, *Salmonella enterica*, *Staphylococcus aureus*, *Escherichia Coli* and *Pseudomonas aeruginosa* were about 10 mm, 14 mm, 8 mm, 8 mm and 10 mm, respectively. The high abundance of amines on their cell surface enhances the affinity of Cu ions towards these groups,^[66] which gives rise to high antimicrobial proficiency of synthesized **Cu-4AP-Br** compound. Similar results were previously reported by Samanta *et al.*^[67] In fact, pyridine-2-carboxamide copper complexes possess good antibacterial activity. Inspection of the data given in Table 5 reveals that **Cu-4AP-Br** is active towards the five tested strain. On the other hand, bacitracin did not show inhibition against *Salmonella enterica*. It was reported that the antibacterial activity of the compound is affected by different factors such as the

TABLE 5 Antibacterial activity of **Cu-4AP-Br** and Bacitracin (C) using agar disc diffusion

	<i>Micrococcus luteus</i>	<i>Salmonella enterica</i>	<i>Staphylococcus aureus</i>	<i>Escherichia Coli</i>	<i>Pseudomonas aeruginosa</i>
IZD (Cu-4AP-Br)	10	14	8	8	10
IZD (C)	19	-	25	9	9

nature of the chelating agent and its chelating sites, the nature of the metal ion, the geometrical structure of the complex, solubility and other factors.^[68] Recently, Saleemh *et al.* have reported that copper (II) complexes have been found to exhibit prominent antimicrobial and anticancer potential activity by inducing apoptosis.^[69] Bacteria are very strong and have already developed struggle to many regularly used antibiotics. This may pave the way for the exploitation of new drugs.

3.4.3 | Inhibitory effect of 5-LOX

5-LOX inhibition by **Cu-4AP-Br** was reported for the first time in the literature, in this study. Naproxen (NAP) is used as an anti-inflammatory agent with analgesic and antipyretic properties. NAP, known as a potent anti-inflammatory, was used as a standard. The effects of **Cu-4AP-Br** and NAP on inhibition of 5-LOX activity are reported in Table 6. This pure compound has 4.6 times stronger anti-inflammatory activity, at a concentration of 25 µg/ml, when compared to the synthesized compound. The finding revealed that, at a test concentration of 100 µg/ml, Cu-4AP-Br exhibited high anti-inflammatory activity (IP = 54.2 ± 2.08%). A similar trend is observed for copper (II)-ibuprofenato complex.^[70] In fact, inhibition of 5-LOX may proceed via redox or metal-chelating mechanisms, apart from competitive (non-redox) enzyme inhibition.^[71] Sorenson has reported that Cu (II) complexes of clinically used nonsteroidal anti-inflammatory drugs (NSAIDs) are often more potent anti-inflammatory agents than either the parent NSAID drug or the uncomplexed Cu salt.^[72] The synthesized **Cu-4AP-Br** exhibited excellent anti-inflammatory

TABLE 6 Anti-inflammatory activity of **Cu-4AP-Br** and NAP at various concentrations

	Concentration (µg/ml)	Inhibition
NAP	2.5	15.01 ± 0.47
	5	31.64 ± 0.82
	25	95.00 ± 2.3
Cu-4AP-Br	25	20.51 ± 0.7
	50	37.96 ± 0.39
	100	54.20 ± 2.08

Values are given as mean ± SD from triplicate determinations ($n = 3$) **Cu-4AP-Br** and NAP as a positive control.

activity, and accordingly this type of synthesized compound should be considered as potential active agent for drug delivery process.

4 | CONCLUSION

In summary, the structural feature of the new mononuclear copper compound template 4-aminopyridine was investigated. The X-ray diffraction of **Cu-4AP-Br** shows the ideal square-planar geometry of the copper atoms, which are isolated from each other with a Cu---Cu distance equal to 9.599 (16) Å. The structural arrangement of the synthesized compound exhibits a supramolecular network manifested by the hydrogen bonds type N—H---Br/O and C—H---π, yielding their structural stability. In particular, the bromine atoms play a crucial role in constructing 0D supramolecular frameworks because they extend acceptors hydrogen bonding as well as maintain the charge balance of the system. **Cu-4AP-Br** was applied as a catalyst in the Heck coupling reaction under ultrasonic irradiation in various reaction conditions. The results found are very encouraging: the ultrasonic activation generates the selectivity on the external position of styrene with a preference of the *trans* form over *cis*. The yields obtained for a short period of time allow us to consider this complex as an excellent catalyst for this type of reaction. Overall, the present study emphasized the significant role attributed to **Cu-4AP-Br** as a promising source for antioxidant and antibacterial agents.

ORCID

Houcine Naïli  <https://orcid.org/0000-0002-9224-5851>

REFERENCES

- [1] N. Mhadhbi, S. Saïd, S. Elleuch, T. Lis, H. Naïli, *J. Mol. Struct.* **2016**, *1105*, 16.
- [2] S. Said, H. Naïli, T. Bataille, R. P. Herrera, *CrystEngComm* **2016**, *1*, 1.
- [3] A. M. Ben Salah, H. Naïli, M. Arczyński, M. Fitta, *J. Organomet. Chem.* **2016**, *805*, 42.
- [4] G. Li, Y. Xing, S. Song, N. Xu, X. Liu, Z. Su, *J. Solid State Chem.* **2008**, *181*, 2406.
- [5] S. Saïd, R. A. Kolsi, H. Naïli, *J. Organomet. Chem.* **2016**, *809*, 45.

- [6] N. Hfidhi, M. Korb, M. Fitta, E. Čižmár, H. Lang, H. Naili, *Inorg. Chim. Acta* **2019**, *484*, 206.
- [7] N. Hfidhi, O. Kammoun, R. Pelka, M. Fitta, H. Naili, *Inorg. Chim. Acta* **2018**, *469*, 431.
- [8] A. M. Ben Salah, N. Sayari, H. Naili, A. J. Norquist, *RSC Adv.* **2016**, *6*, 59055.
- [9] S. Walha, S. Yahyaoui, H. Naili, T. Mhiri, T. Bataille, *J. Coord. Chem.* **2010**, *63*, 1358.
- [10] M. Tadokoro, H. Kanno, T. Kitajima, H. Shimada-Umemoto, N. Nakanishi, K. Isobe, K. Nakasuji, *Proc. Natl. Acad. Sci. U.S.A.* **2002**, *99*, 4950.
- [11] P. Saxena, R. Murugavel, *ChemistrySelect* **2017**, *2*, 3812.
- [12] S. J. J. Titinchi, G. V. Willingh, H. S. Abbo, R. Prasad, *Cat. Sci. Technol.* **2015**, *5*, 325.
- [13] S. Jain, O. Reiser, *ChemSusChem* **2008**, *1*, 534.
- [14] C. Y. Tsai, B. H. Huang, M. W. Hsiao, C. C. Lin, B. T. Ko, *Inorg. Chem.* **2014**, *53*, 5109.
- [15] A. V. Malkov, I. R. Bexendale, M. Bella, V. Langer, J. Fawcett, D. R. Russell, D. J. Mansfield, M. Valko, P. Kocovsky, *Organometallics* **2001**, *20*, 673.
- [16] N. A. Pulina, F. V. Sobin, A. I. Krasnova, T. A. Yushkova, V. V. Yushkov, P. A. Babushkina, E. B. Mokin, *Pharm. Chem. J.* **2011**, *45*, 275.
- [17] Q. Li, C. Zhang, W. Tan, G. Gu, Z. Guo, *Molecules* **2017**, *22*, 156.
- [18] D. Ben Hassan, W. Rekik, A. Otero-de-la Roza, F. Ben Mefteh, T. Roisnel, T. Bataille, H. Naili, *Polyhedron* **2016**, *119*, 238.
- [19] M. J. Belousoff, M. B. Duriska, B. Graham, S. R. Batten, B. Moubaraki, K. S. Murray, L. Specie, *Inorg. Chem.* **2006**, *45*, 3746.
- [20] J. Yu-Mei, F. Yan, H. Pei-Pei, L. Ming-Xue, C. Qian-Qian, H. Qiu-Xia, *Inorg. Chem. Commun.* **2017**, *86*, 22.
- [21] M. J. Giffin, H. Heaslet, A. Brik, L. Ying-Chuan, G. Cauvi, W. Chi-Huey, E. M. Duncan, J. H. Elder, C. D. Stout, B. E. Torbett, *J. Med. Chem.* **2008**, *51*, 6263.
- [22] S. Samanta, S. Ray, S. Joardar, S. Dutta, *J. Chem. Sci.* **2015**, *127*, 1451.
- [23] R. Strandberg, L. Niinistö, J. Møller, G. Schroll, K. Leander, C.-G. Swahn, *Acta Chem. Scand.* **1973**, *27*, 1004.
- [24] (a) APEX2, Bruker AXS Inc., Madison, WI **2014**. (b) G. M. Sheldrick, *SADABS, Program for Empirical Absorption correction of Area Detector Data; University of Göttingen, Göttingen, Germany* **2000**.
- [25] G. M. Sheldrick, *Acta Cryst* **2008**, *A64*, 112.
- [26] K. Brandenburg, *Diamond. Version 3.2i*, Crystal Impact GbR, Bonn, Germany **2012**.
- [27] I. I. Koleva, T. A. van Beek, J. P. H. Linssen, A. de Groot, L. N. Evstatieva, *Phytochem. Anal.: PCA* **2002**, *13*, 8.
- [28] A. Yildirim, A. Mavi, A. A. Kara, *J. Agric. Food Chem.* **2001**, *49*, 4083.
- [29] P. Bersuder, M. Hole, G. Smith, *J. Am. Oil Chem. Soc.* **1998**, *75*, 181.
- [30] J. R. Tagg, A. R. McGiven, *Appl. Microbiol.* **1971**, *21*, 943.
- [31] J. Bekir, M. Mars, J. P. Souchard, J. Bouajila, *Food Chem. Toxicol.* **2013**, *55*, 470.
- [32] A. Escuer, M. A. S. Goher, F. A. Mautner, R. Vicente, *Inorg. Chem.* **2000**, *39*, 2107.
- [33] A. W. Addison, T. N. Rao, *J. Chem. Soc. Dalton Trans.* **1984**, *7*, 1349.
- [34] Z. Rák, J.-P. Maria, D. W. Brenner, *Mater. Lett.* **2018**, *217*, 300.
- [35] L. Gaijuan, X. Yan, S. Shuyan, X. Ning, L. Xianchun, S. Zhongmin, *J. Solid State Chem.* **2008**, *181*, 2406.
- [36] S. K. Wolff, D. J. Grimwood, J. J. McKinnon, M. J. Turner, D. Jayatilaka, M. A. Spackman, *CrystalExplorer (Version 3.0)*, University of Western Australia, Perth **2012**.
- [37] S. Mohanty, B. Punji, M. S. Balakrishna, *Polyhedron* **2006**, *25*, 815.
- [38] D. Suresh, M. S. Balakrishna, J. T. Mague, *Tetrahedron Lett.* **2007**, *48*, 2283.
- [39] N. Miyaura, A. Suzuki, *Chem. Rev.* **1995**, *95*, 2457.
- [40] R. Martin, S. L. Buchwald, *Acc. Chem. Res.* **2008**, *41*, 1461.
- [41] J. Yorke, L. Wan, A. Xia, W. Zheng, *Tetrahedron Lett.* **2007**, *48*, 8843.
- [42] J. A. Terrett, J. D. Cuthbertson, V. W. Shurtleff, D. W. C. MacMillan, *Nature* **2015**, *524*, 330.
- [43] S. Iyer, V. V. Thakur, *J. Mol. Catal. A: Chemical.* **2000**, *157*, 275.
- [44] P. Zhou, Y. Li, P. Sun, J. Zhou, J. Bao, *Chem. Commun.* **2007**, *1*, 1418.
- [45] A. R. Hajipour, G. Azizi, *Green Chem.* **2013**, *15*, 1030.
- [46] R. Jlassi, A. P. C. Ribeiro, E. C. B. A. Alegria, H. Naili, G. A. O. Tiago, T. Rüffer, H. Lang, F. I. Zubkov, A. J. L. Pombeiro, W. Rekik, *Inorg. Chim. Acta* **2018**, *471*, 658.
- [47] C. Zhang, C. Tanga, N. Jiao, *Chem. Soc. Rev.* **2012**, *41*, 3464.
- [48] S. V. Sancheti, P. R. Gogate, *Ultrason. Sonochem.* **2018**, *40*, 30.
- [49] S. Dehghani, M. Haghghi, *Ultrason. Sonochem.* **2017**, *35*, 142.
- [50] E. A. Neppiras, B. E. Noltingk, *Proc. Phys. Soc.* **1950**, *64*, 674.
- [51] D. Atoui, K. Said, R. Ben Salem, *Turk. J. Chem.* **2017**, *41*, 587.
- [52] K. R. Balinge, P. R. Bhagat, *C. R. Chim.* **2017**, *20*, 773.
- [53] X. Jiang, P. Boehm, J. F. Hartwig, *J. Am. Chem. Soc.* **2018**, *140*, 1239.
- [54] A. Shafir, P. A. Lichtor, S. L. Buchwald, *J. Am. Chem. Soc.* **2007**, *129*, 3490.
- [55] H. Wang, H. Zhang, L. Tang, H. Chen, C. Wu, M. Zhao, Y. Yang, X. Chen, G. Liu, *Toxicology* **2013**, *303*, 139.
- [56] A. Molnar, *Chem. Rev.* **2011**, *111*, 2251.
- [57] C. Marzano, M. Pellei, F. Tisato, C. Santini, *Anti Cancer Agents Med. Chem.* **2009**, *9*, 185.
- [58] E. Wieslander, L. Engman, E. Svensjö, M. Erlansson, U. Johansson, M. Linden, R. Brattsand, *Biochem. Pharmacol.* **1998**, *55*, 573.
- [59] İ. Gülçin, *Chem. Biol. Interact.* **2009**, *179*, 71.
- [60] M. Hazra, T. Dolai, A. Pandey, S. K. Dey, A. Patra, *Bioinorg. Chem. Appl.* **2014**, *3*, 1.
- [61] C. Sulpizio, S. T. R. Müller, Q. Zhang, L. Brecker, A. Rompel, *Monatsh. Chem.* **2016**, *147*, 1871.

- [62] K. Konarikova, L. Andrezalova, P. Rapta, M. Slovakova, Z. Durackova, L. Laubertova, H. Gbelcova, L. Danisovic, D. Bohmer, T. Ruml, M. Sveda, I. Zitnanova, *Eur. J. Pharmacol.* **2013**, *721*, 178.
- [63] P. S. Nayak, B. Narayana, B. K. Sarojini, S. Sheik, K. S. Shashidhara, K. R. Chandrashekar, *J. Taibah Univ. Sci.* **2016**, *10*, 823.
- [64] K. Shimada, K. Fujikawa, K. Yahara, T. Nakamura, *J. Agric. Food Chem.* **1992**, *40*, 945.
- [65] N. Sreeju, A. Rufus, D. Philip, *J. Mol. Liq.* **2017**, *242*, 690.
- [66] D. Le Cerf, F. Irinei, G. Muller, *Carbohydr. Polym.* **1990**, *13*, 375.
- [67] S. Samanta, S. Ray, S. Joardar, S. Dutta, Z. Naturforsch, *B: Chem. Sci.* **2015**, *127*, 1451.
- [68] M. Shebl, *J. Mol. Struct.* **2017**, *1128*, 79.
- [69] F. A. Saleemh, S. Musameh, A. Sawafta, P. Brandao, C. J. Tavares, S. Ferdov, I. Warad, *Arab. J. Chem.* **2017**, *10*, 845.
- [70] A. Andrade, S. F. Namora, R. G. Woisky, G. Wiesel, R. Najjar, J. A. Sertié, D. de Oliveira Silva, *J. Inorg. Biochem.* **2000**, *81*, 23.
- [71] R. M. McMillan, E. R. Walker, *Trends Pharmacol. Sci.* **1992**, *13*, 323.
- [72] J. R. J. Sorenson, *J. Med. Chem.* **1976**, *19*, 135.

How to cite this article: Hfidhi N, bkhairia I, Atoui D, et al. Catalytic and biological valorization of a supramolecular mononuclear copper complex based 4-aminopyridine. *Appl Organometal Chem.* 2019;e4793. <https://doi.org/10.1002/aoc.4793>